Acta Crystallographica Section D
Biological Crystallography
ISSN 0907-4449

Crystallization of a member of the recFOR DNA repair pathway, RecO, with and without bound oligonucleotide

Shelly Aono,[a] Thomas Hartsch[b]† and Ursula Schulze-Gahmen[a]*

[a]Physical Biosciences Division at E. O. Lawrence Berkeley National Laboratory, Berkeley, California 94720, USA, and [b]Göttingen Genomics Laboratory, Georg-August-Universität, Göttingen, Germany

† Current address: Integrated Genomics, Winzlaer Strasse 2a, D-07745 Jena, Germany.

Correspondence e-mail: uschulze-gahmen@lbl.gov

Received 30 September 2002
Accepted 3 January 2003

RecFOR proteins are important for DNA repair by homologous recombination in bacteria. The RecO protein from *Thermus thermophilus* was cloned and purified, and its binding to oligonucleotides was characterized. The protein was crystallized alone and in complex with a 14-mer oligonucleotide. Both crystal forms grow under different crystallization conditions in the same space group, $P3_121$ or $P3_221$, with almost identical unit-cell parameters. Complete data sets were collected to 2.8 and 2.5 Å for RecO alone and for the RecO–oligonucleotide complex, respectively. Visual comparison of the diffraction patterns between the two crystal forms and calculation of an $R_{\rm merge}$ of 33.9% on F indicate that one of the crystal forms is indeed a complex of RecO with bound oligonucleotide.

1. Introduction

Maintenance of genomic integrity is extremely important for all organisms. Thus, all cells are equipped with DNA-repair mechanisms for different types of DNA damage. UV irradiation produces pyrimidine dimers which inhibit DNA polymerases and hence DNA replication. *Escherichia coli* has various ways to deal with dimers (Sancar & Sancar, 1988). They can be directly reversed by photo-reactivation catalyzed by photolyase or they can be removed by UvrABC-catalyzed excision repair. The effect of the remaining dimers can be overcome during DNA replication using two recombinational DNA-repair mechanisms (Kowalczykowski *et al.*, 1994; Cox, 1998). The first is the RecBCD-dependent double-strand break repair pathway. The second is RecFOR-dependent post-replication gap repair, which involves homologous recombination. The function of the *recFOR* pathway of recombination is currently not well understood. In *E. coli*, the *recFOR* pathway contributes only 0.1–1% of the recombinational activity in the cell (Horii & Clark, 1973) and *recF* and *recR* mutants have relatively subtle phenotypes with regard to recombination. Their UV sensitivity is, however, greatly increased. Studies by Courcelle *et al.* (1997) suggested that *recF* and *recR* are required for the resumption of replication at stalled DNA-replication forks. Hence, the primary function of proteins in the *recFOR* pathway in *E. coli* may not be recombination, but resumption of DNA replication from existing replication forks. Interestingly, the genome of the closely related bacterium *Deinococcus radiodurans*, the most radiation-resistant organism known, does not include genes for homologues of the *E. coli* RecB and RecC proteins (Makarova *et al.*, 2001). Hence, the *recFOR* pathway could potentially replace some of the RecBCD function in *D. radiodurans*.

In order to obtain a better understanding of the molecular function of proteins in the *recFOR* pathway of homologous recombination, *recF*, *recO* and *recR* genes from *Thermus thermophilus* were cloned for overexpression in *E. coli*. RecO has been purified and crystallized for structural studies. In addition, purified protein was characterized with respect to DNA binding and a complex of RecO with a DNA oligomer was crystallized.

2. Protein expression and purification

The *T. thermophilus* open reading frame (ORF) encoding the RecO protein was identified by homology searches of the genome using the protein sequences for RecO from *D. radiodurans* and *E. coli* as probes. BLAST searches clearly identified a *T. thermophilus* ORF with 28 and 21% amino-acid identity with RecO from *D. radiodurans* and *E. coli*, respectively. The *T. thermophilus recO* gene codes for a 24.6 kDa protein with a theoretical pI of 10.1.

The *T. thermophilus recO* gene was PCR-amplified from genomic DNA. The high GC content (>70%) of the *T. thermophilus* genome required special protocols for the polymerase chain reaction (PCR) procedures. PCR primers were designed to have a melting temperature of at least 343 K and included a 5′ *Nde*I or 3′ *Bam*H1 restriction site. The LA PCR kit, version 2.1, from Takara Shuzo (Shiga, Japan) with a special buffer for GC-rich templates was used for the PCR reaction. The

best results were obtained with the following reaction cycles: 30 s denaturation at 367 K, 30 s annealing at 331 K and 2 min extension at 345 K. The PCR product was gel-purified, ligated into the high-copy pCR 2.1 TOPO vector from the TOPO TA Cloning kit (Invitrogen, Carlsbad, CA, USA) and transformed into Top10 cells. DNA sequencing verified the correct sequence for the *recO* clone. The TOPO vector with the *recO* insert was subsequently digested with *Nde*I and *Bam*H1 and the insert subcloned into the pSKB3 expression vector (a gift from Stephen K. Burley) which encodes an N-terminal hexahistidine tag with a TEV cleavage site (Parks *et al.*, 1994). RecO-pSKB3 was transformed into *E. coli* strain Rosetta/pLysS (Novagen, Madison, WI, USA) for protein expression.

Rosetta/pLysS cells transformed with pSKB3-recO were induced with 0.5 m*M* isopropyl β-D-thiogalactoside (IPTG) at 310 K for 3 h in LB medium containing 50 µg ml^{-1} kanamycin and 34 µg ml^{-1} chloramphenicol. A 1 l culture was harvested by centrifugation and sonicated in 40 ml 50 m*M* Tris, 300 m*M* NaCl pH 7.5 (buffer *A*) with DNAse I (7.5 µg ml^{-1}) and protease inhibitors leupeptin (1 µg ml^{-1}), aprotinin (2 µg ml^{-1}), pepstatin (1 µg ml^{-1}) and PMSF (170 µg ml^{-1}). The lysate was centrifugated at 223 000*g* for 1 h. The supernatant was incubated with 7 ml of Talon IMAC resin (Clontech, Palo Alto, CA, USA) for 1 h and subsequently packed into a gravity-flow column. The resin was washed with buffer *A* followed by stepwise elution with buffer *A* containing 300 m*M* imidazole. The protein was digested with recombinant tobacco etch virus (rTEV) protease (Parks *et al.*, 1994) to remove the histidine tag and purified over a 1.6 ml Poros HS-20 cation-exchange column (Applied Biosystems, Foster City, CA, USA) using a 0–1 *M* NaCl salt gradient in 25 m*M* HEPES pH 7.4, 1 m*M* EDTA. RecO eluted from the column in a single peak at about 700 m*M* NaCl. SDS–PAGE of the protein-containing fractions showed a single band of 25 kDa molecular weight, as expected for *T. thermophilus* RecO. The peak fractions were pooled and the buffer was exchanged to 25 m*M* HEPES pH 7.5, 1 m*M* EDTA, 100 m*M* NaCl. The purified protein was concentrated to about 10 mg ml^{-1} and stored at 277 K. Determination of the molecular weight of RecO by electrospray iontrap mass spectroscopy revealed a molecular weight of 24 842.20 Da, close to the theoretical weight of 24 842.01 Da. Dynamic light-scattering analysis of RecO showed a polydispersity of 15%.

3. RecO binding to DNA

Previous studies of RecO from *E. coli* showed non-sequence-specific binding of RecO to single-stranded (ss) and double-stranded (ds) DNA (Luisi-DeLuca & Kolodner, 1994). In order to analyze the DNA-binding activity of *T. thermophilus* RecO and to identify suitable oligonucleotides for cocrystallization, we probed RecO binding to DNA in various assays.

Gel electrophoresis of RecO protein in 1.5% agarose gels with 90 m*M* Tris–borate pH 8.3 (1 × TB), 10 m*M* $MgCl_2$ buffer showed a decreased mobility for the protein with increasing concentration of a 31-mer oligonucleotide. A molar ratio of 3:1 (oligonucleotide:protein) was necessary to detect a change in protein mobility (Fig. 1).

Purified oligonucleotides for co-crystallization studies were purchased from MWG Biotech Inc. (High Point, NC, USA). The oligonucleotide A14, dATGGACAGCTAGTT, with a molecular weight of 4303 Da was assayed for complex formation with RecO by cation-exchange chromatography on a Poros HS-20 column. Chromatography of RecO alone resulted in a single peak at 280 nm absorption. Separation of RecO incubated with A14 oligonucleotide resulted in two peaks at 280 nm, one identical to RecO alone and an additional earlier eluting peak with a higher absorption at 260 than at 280 nm (Fig. 2). Since the oligonucleotide alone does not bind to the cation-exchange column (data not shown), the peak with the high A_{260}/A_{280} ratio is most likely to be RecO–oligonucleotide complex. The fact that the complex peak is only 5–10% the size of the RecO peak indicates a relatively low affinity of RecO for the oligonucleotide A14, leading to a fairly unstable complex under chromatographic conditions. However, since even low affinities between protein and ligands are sufficient for co-crystallization experiments, A14 was used for co-crystallization with RecO.

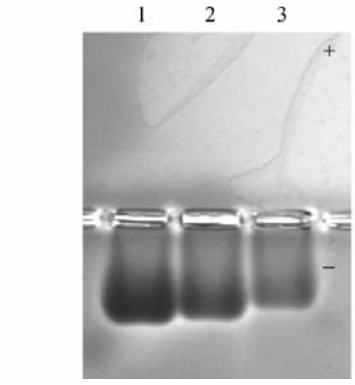

Figure 1
Native agarose-gel electrophoresis of RecO and RecO–oligonucleotide complex. 1 µg RecO was preincubated with a 31-mer oligonucleotide in 1:3 (lane 2) and 1:16 (lane 3) molar ratios in 1 × TB, 10 m*M* $MgCl_2$ for 1 h at 277 K. RecO alone and the preincubated Rec–oligonucleotide mixtures were separated on a 1.5% agarose gel in 1 × TB, 10 m*M* $MgCl_2$. The mobility of RecO alone is reduced by increasing amounts of bound oligonucleotide.

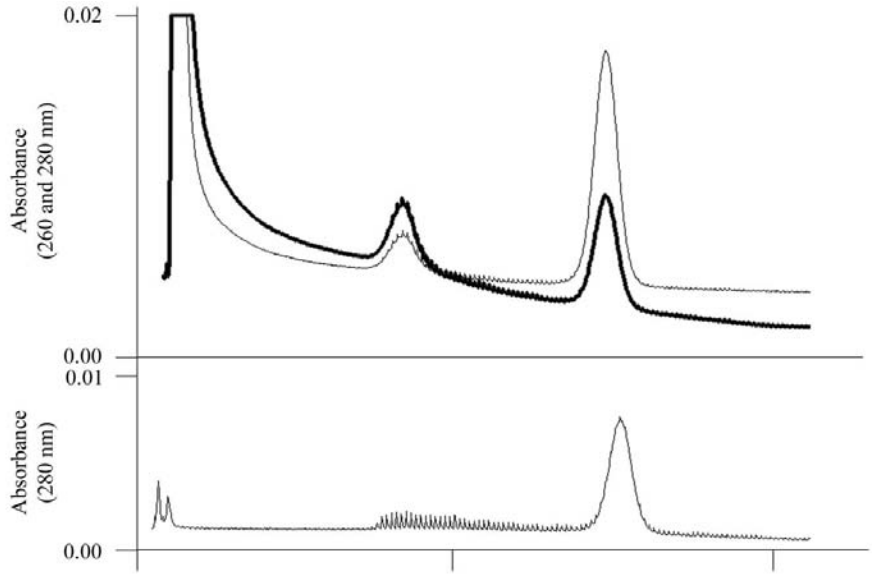

Figure 2
Cation-exchange chromatography of RecO and RecO–oligonucleotide complex. 100 µg RecO was preincubated with 50 µg A14 oligonucleotide for 1 h at 277 K. RecO alone (lower plot) and preincubated RecO–A14 mixture (upper plot) were loaded onto an HS-20 cation-exchange column in 25 m*M* HEPES pH 7.5, 1 m*M* EDTA buffer and eluted with a linear gradient of 0–1 *M* NaCl in the same buffer over 20 column volumes. The absorbance of the eluted molecules was recorded at 280 nm (thin lines) and 260 nm (thick line).

4. Crystallization

RecO was concentrated to 10 mg ml^{-1} in 25 m*M* HEPES pH 7.4, 1 m*M* EDTA, 0.10 *M* NaCl for crystallization experiments using the hanging-drop vapour-diffusion method. Initial screening of crystallization conditions with Crystal Screen I (Hampton Research, Laguna Niguel, CA, USA) resulted in crystals in 0.2 *M* $LiSO_4$, 0.1 *M* Tris–HCl pH 8.5, 30% PEG 4000. These conditions were optimized to yield large single crystals with a trigonal rod shape. In the final crystallization condition, 0.7 µl RecO protein was combined with 0.7 µl 0.15 *M* potassium phosphate, 12.5% PEG 4000, 0.1 *M* Tris pH 9.1 and equilibrated against the precipitant at 295 K. Single crystals with average dimensions of 0.15 × 0.15 × 0.3 mm grew within 4 d (Fig. 3*a*).

For co-crystallization of RecO with the A14 oligonucleotide, RecO at 10 mg ml^{-1} was preincubated for 1 h at 277 K with A14 in a 1:1.7 molar ratio. Initial crystallization conditions were again determined using Crystal Screen I from Hampton Research followed by optimization. In the final crystallization conditions, 0.7 µl RecO–A14 complex was combined with 0.7 µl 0.1 *M* $LiSO_4$, 0.1 *M* Tris pH 8.5, 20% PEG 4000 and equilibrated against the precipitant at 295 K. Single crystals grew in a few days to average dimensions of 0.15 × 0.15 × 0.3 mm. The morphology of the complex crystals is almost indistinguishable from the RecO crystals without oligonucleotide (Fig. 3*b*).

5. Diffraction data collection

Crystals of RecO alone were soaked in the crystallization mother liquor with a stepwise increasing concentration of glycerol from 10 to 30% prior to cryocooling in liquid nitrogen. The cooled crystal was transferred with cryotongs to a nitrogen cold stream at ~100 K. The presumed RecO–A14 complex crystals were cryocooled directly out of the crystallization drop after a gradual increase of the PEG concentration to 28% by vapour diffusion. Complete X-ray data sets from the RecO crystals alone and in complex with the oligonucleotide A14 were collected at the Advanced Light Source (Lawrence Berkeley National Laboratory) beamlines 5.01 and 5.02. The RecO and RecO–oligonucleotide complex crystals diffracted to 2.8 and 2.5 Å, respectively. Autoindexing and examination of the systematic absences in the data indicate that the space group is $P3_121$ or $P3_221$, with similar unit-cell parameters for both crystals (Table 1). Assuming one RecO molecule or RecO–A14 complex per asymmetric unit results in 58% solvent content for the RecO crystal and 51.6% solvent content for RecO–A14 complex crystals. All data were processed using the *HKL* package (Otwinowski & Minor, 1997) and *TRUNCATE* from the *CCP*4 suite (Collaborative Computational Project, Number 4, 1994), resulting in complete data sets of good quality.

Table 1
X-ray data-collection statistics.

Values in parentheses refer to the highest resolution shell.

	RecO alone	RecO–A14 complex
Space group	$P3_121$ or $P3_221$	$P3_121$ or $P3_221$
Unit-cell parameters (Å)	$a = b = 92.8$, $c = 65.8$	$a = b = 93.4$, $c = 65.6$
Resolution range (Å)	20.0–2.8	50.0–2.5
No. of observations	44344	127725
No. of unique reflections	8264	11800
Multiplicity	6.5	10.0
Completeness (%)	99.8 (100.0)	99.5 (98.2)
Average $I/\sigma(I)$	32.6 (6.0)	70.0 (3.6)
R_{sym}† (%)	4.2 (22.5)	7.2 (49.6)
Mosaicity	0.8	1.0

† $R_{sym} = \sum_{hkl} \sum_i |I_i - \langle I \rangle| / \sum \langle I \rangle$, where I_i is the intensity of the ith measurement of reflection hkl and $\langle I \rangle$ is the average intensity of the reflection.

Using the data sets from both RecO crystal forms, pseudo-precession pictures of various reverse lattice planes for both crystals were generated. The diffraction patterns show significant differences, although the space group and the unit-cell parameters are almost identical in both crystals (Figs. 3*c* and 3*d*). The weighted R_{merge} on F between the two data sets is 33.9% for the 20–2.8 Å resolution range. These differences in the diffraction intensities indicate that the RecO crystals grown in the presence of A14 oligonucleotide are indeed composed of RecO–A14 complex molecules.

To determine the structure of the RecO–oligonucleotide complex crystals, RecO was co-crystallized with A14 oligonucleotide with 5-Br-deoxyuracil replacing the usual deoxythymidine. The incorporation of the anomalous scatterer Br into the complex crystals will allow phasing of the diffraction data for structure determination.

This work was funded by a grant from the US Department of Energy Contract No. (DE-AC03-76SF00098). We thank Dr David King for performing mass spectroscopy on RecO and Dr Stephen Holbrook for helpful discussions.

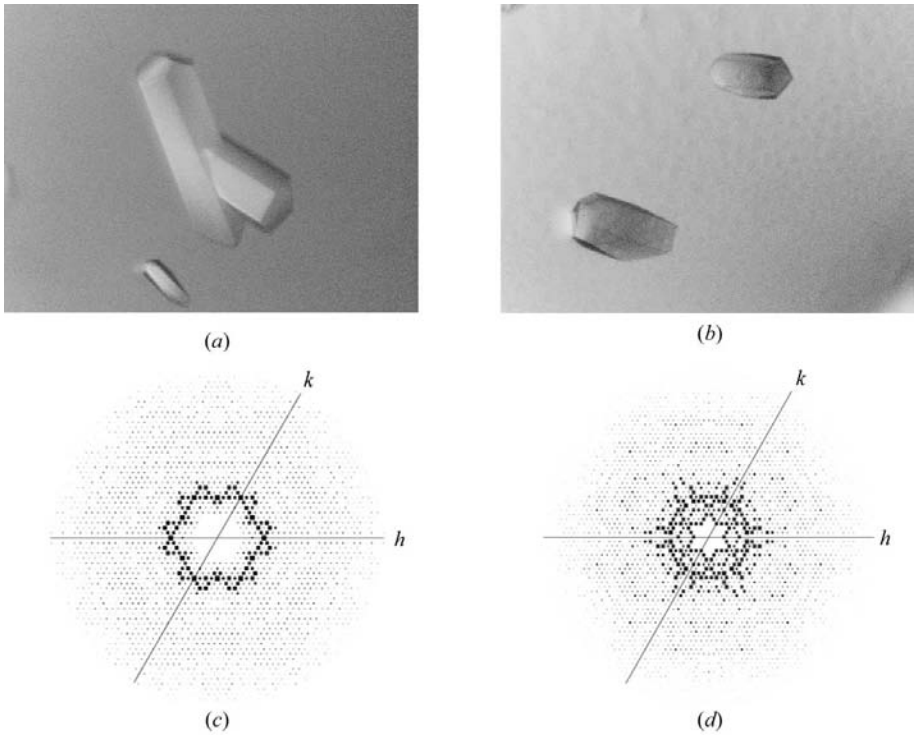

Figure 3
Photographs of RecO crystals and their corresponding diffraction patterns. Crystals of RecO alone are shown in (*a*), with the *hk*0 reciprocal-lattice plane displayed in (*c*). Crystals of RecO in complex with A14 oligonucleotide are shown in (*b*), with the corresponding *hk*0 reciprocal-lattice plane in (*d*). Although the crystal morphologies are very similar, the diffraction patterns are quite different.

References

Courcelle, J., Carswell Crumpton, C. & Hanawalt, P. C. (1997). *Proc. Natl Acad. Sci. USA*, **94**, 3714–3719.

Collaborative Computational Project, Number 4 (1994). *Acta Cryst.* D**50**, 760–763.
Cox, M. M. (1998). *Genes Cells*, **3**, 65–78.
Horii, Z. & Clark, A. J. (1973). *J. Mol. Biol.* **80**, 327–344.
Kowalczykowski, S. C., Dixon, D. A., Eggleston, A. K., Lauder, S. D., Rehrauer, W. M. (1994). *Microbiol. Rev.* **58**, 401–465.
Luisi-DeLuca, C. & Kolodner, R. (1994). *J. Mol. Biol.* **236**, 124–138.
Makarova, K. S., Aravind, L., Wolf, Y. I., Tatusov, R. L., Minton, K. W., Koonin, E. V. & Daly, M. J. (2001). *Microbiol. Mol. Biol. Rev.* **65**, 44–79.
Otwinowski, Z. & Minor, W. (1997). *Methods Enzymol.* **276**, 307–326.
Parks, T. D., Leuther, K. K., Howard, E. D., Johnston, S. A. & Dougherty, W. G. (1994). *Anal. Biochem.* **216**, 413–417.
Sancar, A. & Sancar, G. B. (1988). *Annu. Rev. Biochem.* **57**, 29–67.